

# RSC Advances



This is an *Accepted Manuscript*, which has been through the Royal Society of Chemistry peer review process and has been accepted for publication.

*Accepted Manuscripts* are published online shortly after acceptance, before technical editing, formatting and proof reading. Using this free service, authors can make their results available to the community, in citable form, before we publish the edited article. This *Accepted Manuscript* will be replaced by the edited, formatted and paginated article as soon as this is available.

You can find more information about *Accepted Manuscripts* in the [Information for Authors](#).

Please note that technical editing may introduce minor changes to the text and/or graphics, which may alter content. The journal's standard [Terms & Conditions](#) and the [Ethical guidelines](#) still apply. In no event shall the Royal Society of Chemistry be held responsible for any errors or omissions in this *Accepted Manuscript* or any consequences arising from the use of any information it contains.

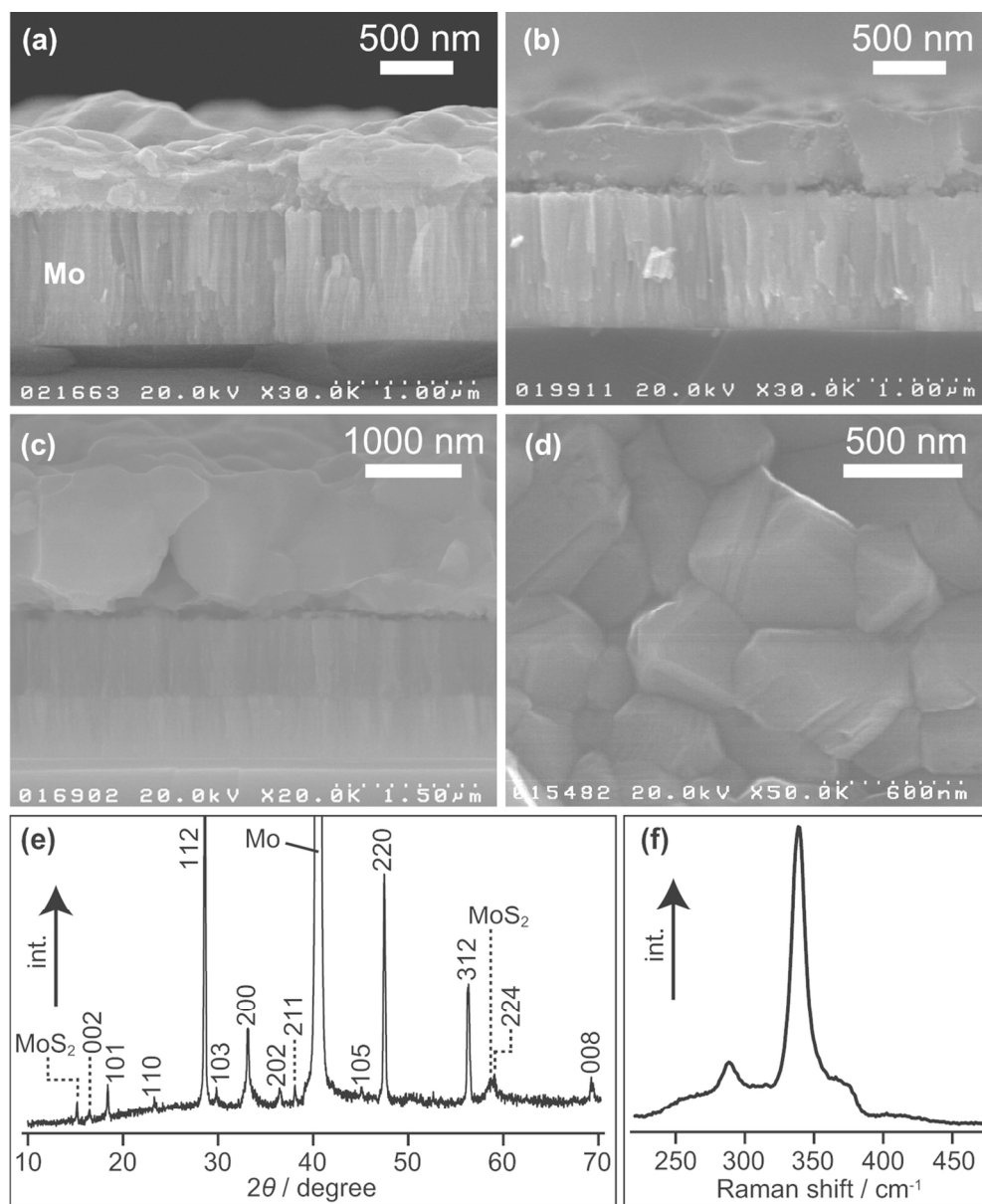


Figure 1  
114x139mm (300 x 300 DPI)

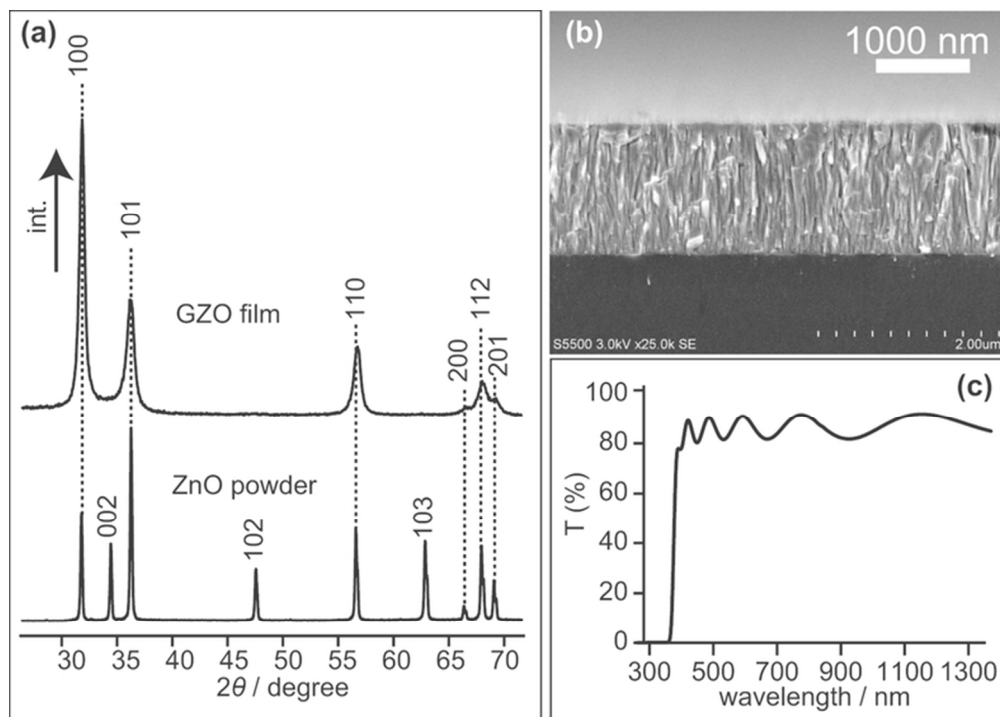


Figure 2  
66x47mm (300 x 300 DPI)

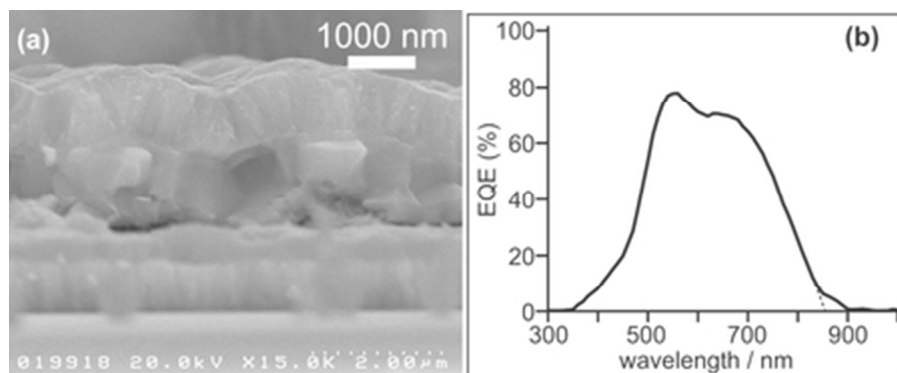
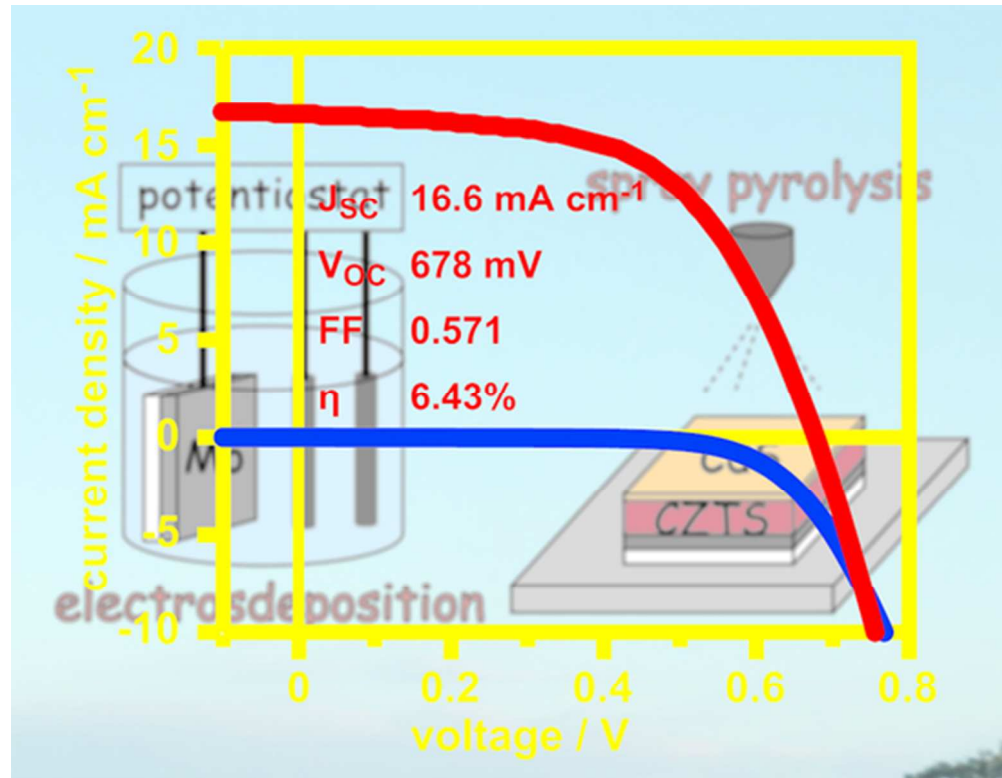


Figure 3  
37x15mm (300 x 300 DPI)



46x35mm (300 x 300 DPI)

Fabrication of an efficient electrodeposited  $\text{Cu}_2\text{ZnSnS}_4$ -based solar cells with more than 6% conversion efficiency using a sprayed Ga-doped ZnO window layer

*Feng Jiang,<sup>a</sup> Shigeru Ikeda,<sup>a\*</sup> Takashi Harada,<sup>a</sup> Akiko Ide,<sup>b</sup> Akiko Mochihara,<sup>b</sup> Kenji Yoshino,<sup>b</sup> Michio Matsumura<sup>a</sup>*

### **Broader context**

A  $\text{Cu}_2\text{ZnSnS}_4$  (CZTS) thin film is a sustainable alternative of a photoabsorber layer in thin-film solar cells because of its earth abundant composition and desirable optical/electrical properties. Among the various methods for fabrication of a CZTS thin film, solution-based deposition has been studied for providing low-cost scalable routes: indeed, several successful examples of efficient devices were reported using CZTS thin films obtained by various solution-based methods. For the fabrication of a complete solar cell device in such CZTS-based solar cells, however, a vacuum-deposited transparent conductive oxide (TCO) was often employed as a front contact window layer. Since the CZTS/CdS heterojunction degrades upon heating it at a temperature above 200 °C, the TCO layer should be deposited at a temperature less than 200 °C. The difficulty in obtaining a high-performance TCO thin film using conventional non-vacuum approaches at such low temperature ranges impedes the application of a non-vacuum deposited TCO to the CZTS-based solar cell. In this study, we successfully utilized a spray-processed Ga-doped ZnO (GZO) layer grown at 100 °C as the front electrical contact in a CZTS-based thin film device prepared by an electrodeposition technique. The device thus-obtained exhibited the best conversion efficiency of 6.43%.

## Abstract

By the combination of electrochemical deposition of a high-quality  $\text{Cu}_2\text{ZnSnS}_4$  (CZTS) thin film photoabsorber and low-temperature spray deposition of Ga-doped ZnO (GZO) transparent conductive oxide, we fabricated a non-vacuum-processed CZTS solar cell. Despite various unoptimized parameters for the TCO layer, such as deposition temperatures and control of film thicknesses, we could obtain the best conversion efficiency of 6.43% with a short circuit current density, an open circuit voltage and a fill factor of  $16.6 \text{ mA cm}^{-2}$ , 678 mV and 0.571, respectively.

Thin film compound semiconductors such as  $\text{Cu}(\text{In,Ga})\text{Se}_2$ (CIGS) and CdTe are currently used as photoabsorbers of thin film solar cells owing to their advantages of high conversion efficiencies.<sup>1-3</sup> Nevertheless, high costs of the rare constituent elements of In and Te limit production and applications of CIGS- and CdTe-based solar cells. Kesterite thin films such as  $\text{Cu}_2\text{ZnSnS}_4$  (CZTS) and  $\text{Cu}_2\text{ZnSn}(\text{S,Se})_4$  (CZTSSe) are considered as potential alternatives to the above traditional chalcogenide-based thin film solar cells because of their earth-abundant constituents.<sup>4-30</sup> The pure sulfide Kesterite, CZTS, has a relatively wide band gap of 1.5eV and a large absorption coefficient of  $10^5 \text{ cm}^{-1}$ .<sup>4</sup> Although current conversion efficiencies of CZTS-based solar cells are slightly lower than those of analogous CZTSSe-based solar cells, development of CZTS-based solar cells is attractive since they do not contain the toxic Se component, i.e., they should contribute to appreciable reductions of manufacturing costs in the feature production process. Hence, several approaches for preparation of CZTS thin films, e.g., evaporation,<sup>4,5</sup> sputtering,<sup>6,7</sup> painting,<sup>8-13</sup> and electrodeposition,<sup>14-19</sup> have been studied. Among them, electrodeposition has been proved to be a promising method because of its cost effectiveness, e.g., low equipment cost, negligible waste of chemicals with utilization efficiencies close to 100%, possible formation of a compact film required for solar cell application, scalability, and manufacturability of a large-area polycrystalline film. After the work reported by A. Ennaoui and co-workers in 2009,<sup>14</sup> photovoltaic performance of electrodeposited CZTS-based solar cells has made rapid progress, and several milestone

results have been reported. In 2012, a solar cell with the best conversion efficiency of 7.3% at the time was reported by using a CZTS thin film obtained by sulfurization of an electrodeposited metallic stack composed of Cu, Sn and Zn layers.<sup>16</sup> Based on studies along with these literature works and experiences, we found that preheating of the electrodeposited metallic stack for a long time before sulfurization can significantly improve the efficiency of the CZTS solar cell; an active area efficiency of 8.0% was obtained in our recent study.<sup>19</sup>

As mentioned above, electrodeposition allows the CZTS absorber to be prepared via a non-vacuum approach at a low cost. For the preparation of a thin layer of n-type CdS on the top of the CZTS film to form the CZTS/CdS heterojunction, we can use a non-vacuum chemical bath deposition method. In order to complete the solar cell structure, however, we often employ a vacuum method such as sputtering for deposition of a transparent conductive oxide (TCO) window layer, such as indium tin oxide (ITO) and Al- or Ga-doped ZnO (AZO or GZO), on top of the CdS layer. From the environmental viewpoint, application of a non-vacuum technique should be promising for TCO deposition. However, most of the non-vacuum methods for TCO deposition require a relatively high temperature ( $> 300\text{ }^{\circ}\text{C}$ ). As has been observed on the CIGS/CdS heterojunction,<sup>31</sup> the CZTS/CdS heterojunction can degrade due probably to Cd diffusion when annealing it at high temperatures.<sup>32</sup> Therefore, almost all of the reported CZTS-based solar cells (as well as CZTSSe-based solar cells) have so far been prepared by using sputtered TCO window layers; there is only example of appreciable efficiency of 3.6% using a sol-gel prepared AZO window layer for a CZTS-based solar cell.<sup>12</sup>

Recently, one of the authors (KY) has developed a method of successful growth of a high-quality transparent GZO film by a conventional atmospheric spray pyrolysis at low temperatures ( $< 150\text{ }^{\circ}\text{C}$ ) using diethylzinc (DEZ) triethylgallium (TEG) diluted with diisopropyl ether.<sup>33,34</sup> Moreover, the GZO film was shown to be applicable for a TCO layer of the thin film solar cell based on a  $\text{Cu}(\text{In,Ga})\text{Se}_2$  (CIGS) photoabsorber fabricated by the conventional three-stage evaporation process: the efficiency of the thus-obtained device was 10.4%.<sup>35</sup> In the present study, therefore, we attempted to fabricate a CZTS-based solar cell by utilizing the above low-temperature and non-vacuum processed GZO thin film.



Fig. 1a shows a cross-sectional SEM image of the electrodeposited Cu-Zn-Sn metallic stack used in this study. The metallic precursor appears to be homogeneous covered on the top of the Mo layer. A stacked morphology is slightly observed though it is difficult to distinguish each metallic layer. When the sample was annealed at 310 °C for 2.5 h in an evacuated Pyrex ampoule, the stacked morphology was changed to be a bulk structure without any obvious interfaces, as shown in Fig. 1b. The annealing treatment induces formation of Cu-Zn and Cu-Sn binary alloys; this treatment is essential to obtain a CZTS film adequate for solar cell application.<sup>18,19</sup> Cross-sectional and top-view SEM images of the CZTS film obtained after sulfurization of the annealed metallic precursor are shown in Figs. 1c and 1d. A compact film with large grains was obtained, as expected. It is noted that the cross-section clearly indicate darkening of the upper part of the Mo layer due to the formation of MoS<sub>2</sub> during sulfurization in the present condition.<sup>18</sup> As shown in Fig. 1e, the corresponding XRD pattern was in good agreement with that of the kesterite CZTS compound (PDF No. 57-0575). In addition to the CZTS reflections, moreover, diffraction peaks assignable to metallic Mo and MoS<sub>2</sub> phases were also observed, indicating partial sulfurization of the Mo back contact as mentioned by the above SEM result. Fig. 1f shows Raman spectrum of the sulfurized film. The stronger peak at 337-338 cm<sup>-1</sup> can be assigned to the A vibrational mode from the kesterite CZTS.<sup>6,16,19,36</sup> The weaker peak at 287-288 cm<sup>-1</sup> and broad shoulder bands at around 235-265 cm<sup>-1</sup> and 364-388 cm<sup>-1</sup> are also derived from CZTS, similar to results reported in the literature.<sup>6,16,19,36</sup> Additional very weak peaks at 303-304cm<sup>-1</sup> and 314-315cm<sup>-1</sup> might be attributed to presences of tiny amounts of cubic Cu<sub>2</sub>SnS<sub>3</sub> and SnS<sub>2</sub>, respectively.<sup>37,38</sup> Another broad band at 390-440 cm<sup>-1</sup> is likely to be derived from MoS<sub>2</sub>, as suggested by the XRD result.

As discussed previously,<sup>19</sup> there was significant dependence of solar cell property on duration of the 310-°C annealing, i.e., the longer the annealing duration was, the higher the conversion efficiency was. Provisional assignments of XRD patterns of metallic precursors after the annealing treatment for 40 min and 150 min indicate an appreciable decrease in the Sn component with increase in the annealing duration: as a result, the final CZTS film obtained after the 150-min annealing showed relatively long carrier lifetime as measured by

the time-resolved photoluminescence analyses (data not shown). Hence, sufficient interdiffusion and homogenization of Cu, Zn and Sn components before the sulfurization should be essential to improve the quality of the final CZTS film. Although the details in mechanistic aspects of the growth mechanism and dependence of the quality on the 310-°C annealing duration would be discussed elsewhere, we employed relatively longer annealing duration (2.5 h) in this study.

Fig. 2a shows an XRD pattern of the GZO film grown on a glass substrate by the present atmospheric spray pyrolysis at 100 °C. An XRD pattern of ZnO powder is also shown for comparison. The GZO film showed three intense diffraction peaks at 28.58°, 47.48° and 56.35°, which are assignable to (100), (101), and (110) reflections of hexagonal ZnO. Compared to the XRD pattern of the powder sample, the (100) reflection is dominant, indicating preferential orientation along the *a*-axis. As shown in Fig. 2b, the corresponding cross-sectional SEM image indicates that a compact columnar crystal is grown to form a significantly flat morphology: thickness of the film in the present conditions is about 1300 nm. Optical transmittance of the GZO film is shown in Fig. 2c. A fundamental absorption is clearly observed at a wavelength shorter than ca. 360 nm, implying good crystallization of the sample. The appreciable vibration of the spectrum is interference between the glass substrate and the GZO film, as expected from the film thickness and flatness. There is no drop of the total transmittance in the NIR wavelength range: the average transmittance is clearly above 80%. Electrical resistivity and Hall-effect measurements of the GZO film were carried out by the Van der Pauw's method at ambient temperature. As a result, the lowest resistivity of  $2.3 \times 10^{-3} \Omega \text{ cm}$  was obtained at GZO; carrier concentration and mobility were  $1.1 \times 10^{20} \text{ cm}^{-3}$  and  $10 \text{ cm}^2 (\text{Vs})^{-1}$ , respectively.

Based on the above-mentioned properties, we used the spray-grown GZO as a window layer and front contact in the electrodeposited CZTS-based thin film solar cells with an Al/GZO/CdS/CZTS/Mo/glass structure. Various solar cells were constructed using the same conditions. Fig. 3a shows a typical cross-sectional SEM image of thus-prepared device. Similar to the above GZO film deposited on a glass substrate (see Fig. 2b), more than 1000nm-thick GZO layer was clearly observed on the top part of the film, indicating a

successful complete coverage of bottom CdS and CZTS layers. Table 1 summarizes solar cell parameters obtained by several devices. Except for the worst device (entry 2) derived from the obvious shunting due probably to pinholes in the CZTS film, most of devices showed appreciable solar cell properties. To the best of our knowledge, this is the first time to utilize the spray method to deposit window layers for pure sulfide CZTS solar cells. More than half of the solar cells fabricated exhibited good properties with short circuit current densities ( $J_{SC}$ ), open circuit voltages ( $V_{OC}$ ), and fill factors (FFs) of 16-17  $\text{mAcm}^{-2}$ , 660-0.690 mV and 0.50-0.58, respectively: these cells achieved conversion efficiencies ( $\eta$ s) of more than 5.5%. Moreover, as shown in entries 7 and 8 in Table 1, the champion devices in the present study exhibited conversion efficiency of 6.4%. Since the best conversion efficiency of CZTS-based solar cells based on a non-vacuum processed window layer was 3.6%,<sup>12</sup> the efficiency obtained in this study is the highest value, even though the value is still lower than our best electrodeposited CZTS-based solar cell using a vacuum-sputtered ITO window layer (8.0%).<sup>19</sup> The wavelength dependence of external quantum efficiency (EQE) for the best CZTS solar cell is shown in Fig. 3b. The EQE value of the solar cell is more than 70% in the range of 520-670 nm, but has a gradual decrease along with increase in the wavelength to the band edge (ca. 850 nm, corresponding to the band gap of 1.5 eV). As reported previously for the CZTSSe-based solar cells,<sup>25</sup> the decrease was attributed to the short minority carrier diffusion length of the present CZTS absorber. Moreover, the appreciable existence of Urbach tail at wavelengths longer than the band gap of CZTS (850-900 nm) suggests presences of moderate amounts of sub-gap states near the band edge in the CZTS. In addition, appreciably low parameters were also obtained in some solar cells despite the same procedure being used for device fabrication (entries 1 and 5). Since these devices showed reductions in all of the solar cell parameters, junction qualities of them should be worse than those of devices giving higher  $\eta$  values. Although there is no evidence at present, one of the probable reasons leading to such worse properties is degradation of the p-n junction during GZO deposition because of the exposure to a high temperature environment in an open air for a long duration. Thus, further optimization of deposition conditions is likely to improve not only the reproducibility but also the best  $\eta$  value. These studies are now underway.

## Experimental section

CZTS absorbers were fabricated by sulfurization of preheated electrodeposited Cu-Sn-Zn precursors. Firstly, metallic precursors of Cu, Sn and Zn layers were sequentially electrodeposited on a Mo-coated soda lime glass substrate (Mo/glass) using a conventional three electrode setup consisting of an Ag/AgCl reference electrode, a Pt foil counter electrode and the Mo/glass substrate as a working electrode. The Cu layer was deposited at -0.4 V (vs. Ag/AgCl) using an electroplating bath containing  $\text{CuSO}_4 \cdot 5\text{H}_2\text{O}$  ( $0.05 \text{ mol L}^{-1}$ ), citric acid ( $0.02 \text{ mol L}^{-1}$ ) and trisodium citrate ( $0.04 \text{ mol L}^{-1}$ ). The Sn layer was deposited at -0.54 V (vs. Ag/AgCl) using a bath containing Sn(II) methanesulfonate ( $0.05 \text{ mol L}^{-1}$ ), methanesulfonic acid ( $1 \text{ mol L}^{-1}$ ) and Empigen® BB detergent (*n*-dodecyl-N,N-dimethylglycine,  $1 \text{ mol L}^{-1}$ ). The Zn layer was deposited at -1.2 V (vs. Ag/AgCl) using a bath solution containing  $\text{ZnSO}_4 \cdot 7\text{H}_2\text{O}$  ( $0.1 \text{ mol L}^{-1}$ ) and  $\text{K}_2\text{SO}_4$  ( $0.5 \text{ mol L}^{-1}$ ) with pH adjusted to 3 using a HYDRON® buffer. The thus-obtained Cu-Zn-Sn metallic stack was annealed at  $310 \text{ }^\circ\text{C}$  for 2.5 h in an evacuated Pyrex ampoule with a volume of ca.  $5 \text{ cm}^3$ . Then the annealed metallic precursor was sulfurized in a  $590 \text{ }^\circ\text{C}$ -heated furnace with sulfur powder for 10 min to obtain the CZTS film. For use as a solar cell, a 90-nm-thick CdS layer was deposited on the thus-obtained CZTS film using an aqueous deposition method as reported previously.<sup>18,19</sup>

A home-made spray pyrolysis setup was used for deposition of the GZO film. Details of the equipment were described previously.<sup>33-35</sup> Onto a glass substrate made of quartz, DEZ and TEG diluted with diisopropyl ether (supplied by Tosoh Finechem Corporation) were sprayed using  $\text{N}_2$  as a carrier gas. In this study, a novel precursor having a Zn-O structure was synthesized for GZO film deposition by the reaction of diethylzinc and water in some ethersolvents.<sup>39</sup> The weight ratio of DEZ to TEG was fixed to be 1 to 5: this results in 2wt% Ga content in the final film. The substrate temperature and deposition duration were fixed at  $100 \text{ }^\circ\text{C}$  and 24 min, respectively. After the deposition, the resulting film was exposed to UV radiation using a 4 W black light for 60 min. The UV treatment is effective for reducing the resistivity.<sup>33,34</sup> The spray deposition of GZO was also performed on the CdS-modified CZTS film by using the same procedure: the thus-obtained stacked layer of

GZO/CdS/CZTS/Mo/glass was used as a solar cell after deposition of a 500-nm-thick Al collection grid by thermal evaporation.

Crystalline structures of CZTS and GZO films were analyzed by using a Rigaku Mini Flex X-ray diffract meter (Cu K $\alpha$ , Ni filter). A JASCO NRS-3100 Laser Raman Spectrophotometer was also used to examine the structure of the CZTS film. Morphologies of these films were examined using a Hitachi S-5000 field emission scanning electron microscope (FE-SEM) and a Hitachi S-5500FE-SEM at a voltage of 20 kV. Optical transmittance of the GZO film was measured at room temperature using a JASCOV-670 spectrophotometer. Hall-effect measurement of the GZO film was also carried out at room temperature using the Van der Pauw's technique by using a Toyo 8300 Hall-effect and resistivity measurement system. Current density-voltage characteristics of the solar cells were measured in air with a Bunkoh-Keiki CEP-015 photo-voltaic measurement system under a simulated amplitude modulation of AM 1.5G irradiation (100 mW cm<sup>-2</sup>).

### Acknowledgements

This work was carried out as part of a program supported by NEDO Japan. This work was also supported by the A-step feasibility study program from JST Japan and a Grant-in-Aid for Scientific Research on Innovative Areas (All Nippon Artificial Photosynthesis Project for Living Earth) from MEXT Japan.

### Notes and references

<sup>a</sup>Research Center for Solar Energy Chemistry, Osaka University, 1-3 Machikaneyama, Toyonaka, Osaka 560-8531, Japan. Fax: +81-6-6850-6699; Tel: +81-6-6850-6696; E-mail: siked@chem.es.osaka-u.ac.jp

<sup>b</sup>Department of Applied Physics and Electronic Engineering, University of Miyazaki, 1-1 Gakuen Kibanadai-nishi, 889-2192 Miyazaki, Japan.

- 1 P. Jackson, D. Hariskos, E. Lotter, S. Paetel, R. Wuerz, R. Menner, W. Wischmann and M. Powalla, *Prog. Photovolt: Res. Appl.*, 2011, **19**, 894-897.

- 2 A. Chiril, S. Buecheler, F. Pianezzi, P. Bloesch, C. Gretener, A. R. Uhl, C. Fella, L. Kranz, J. Perrenoud, S. Seyrling, R. Verma, S. Nishiwaki, Y. E. Romanyuk, G. Bilger and A. N. Tiwari, *Nat. Mater.*, 2011, **10**, 857-861.
- 3 M. Gloeckler, I. Sankin and Z. Zhao, *IEEE J. Photovolt.*, 2013, **3**, 1389-1393.
- 4 H. Katagiri, K. Saitoh, T. Washio, H. Shinohara, T. Kurumadani and S. Miyajima, *Sol. Energy Mater. Sol. Cells*, 2001, **65**, 141-148.
- 5 A. Redinger, D. M. Berg, P. J. Dale and S. Siebentritt, *J. Am. Chem. Soc.*, 2011, **133**, 3320-3323.
- 6 H. Katagiri, K. Jimbo, S. Yamada, T. Kamimura, W. S. Maw, T. Fukano, T. Ito and T. Motohiro, *Appl. Phys. Express*, 2008, **1**, 041201.
- 7 J. J. Scragg, T. Kubart, J. T. Watjen, T. Ericson, M. K. Linnarsson and C. Platzer-Bjorkman, *Chem. Mater.*, 2013, **25**, 3162-3171.
- 8 K. Woo, Y. Kim and J. Moon, *Energy Environ. Sci.*, 2012, **5**, 5340-55345.
- 9 H. Duan, W. Yang, B. Bob, C. Hsu, B. Lei and Y. Yang, *Adv. Funct. Mater.*, 2013, **23**, 1466-1471.
- 10 R. Mainz, B.C. Walker, S.S. Schmidt, O. Zander, A. Weber, H. Rodriguez-Alvarez, J. Just, M. Klaus, R. Agrawal and T. Unold, *Phys. Chem. Chem. Phys.*, 2013, **15**, 18281-18289.
- 11 R. Mainz, A. Singh, S. Levchenko, M. Klaus, C. Genzel, K.M. Ryan and T. Unold, *Nat. Commun.*, 2014, **5**, 3133, doi: 10.1038/ncomms4133
- 12 T. Aizawa, K. Tanaka, K. Tagami and H. Uchiki, *Phys. Status Solidi C*, 2013, **10**, 1050-1054.
- 13 H. Zhou, H. Duan, W. Yang, Q. Chen, C. Hsu, W. Hsu, C. Chen and Y. Yang, *Energy Environ. Sci.*, 2014, **7**, 998-1005.
- 14 A. Ennaoui, M. Lux-Steiner, D. Abou-Ras, I. Kotschau, H.-W. Schock, R. Schurr, A. Holzing, S. Jost, R. Hock, T. Voss, J. Schulze and A. Kribs, *Thin Solid Films*, 2009, **517**, 2511-2514.
- 15 J. J. Scragg, D. Berg, and P. J. Dale, *J. Electroanal. Chem.*, 2010, **646**, 52-59.

- 16 S. Ahmed, K. B. Reuter, O. Gunawan, L. Guo, L. T. Romankiw and H. Deligianni, *Adv. Energy Mater.*, 2012, **2**, 253-259.
- 17 P. Sarswat and M. L. Free, *J. Electron. Mater.*, 2012, **41**, 2210-2215.
- 18 Y. Lin, S. Ikeda, W. Septina, T. Harada and M. Matsumura, *Sol. Energy Mater. Sol. Cells*, 2014, **120**, 218-225.
- 19 F. Jiang, S. Ikeda, T. Harada and M. Matsumura, *Adv. Energy Mater.*, 2014, **4**, 1301381.
- 20 Q. Guo, H. W. Hillhouse and R. Agrawal, *J. Am. Chem. Soc.*, 2009, **131**, 11672-11673.
- 21 T. K. Todorov, K. B. Reuter and D. B. Mitzi, *Adv. Mater.*, 2010, **22**, E156-E159.
- 22 W. Yang, H.-S. Duan, B. Bob, H. Zhou, B. Lei, C.-H. Chung, S.-H. Li, W. W. Hou, Y. Yang, *Adv. Mater.*, 2012, **24**, 6323-6329.
- 23 I. Repins, C. Beall, N. Vora, C. DeHart, D. Kuciauskas, P. Dippo, B. To, J. Mann, W.-C. Hsu, A. Goodrich and R. Noufi, *Sol. Energy Mater. Sol. Cells*, 2012, **101**, 154-159.
- 24 Y. Cao, M. S. Denny, J. V. Caspar, W. E. Farneth, Q. Guo, A. S. Ionkin, L. K. Johnson, M. Lu, I. Malajovich, D. Radu, H. D. Rosenfeld, K. R. Choudhury and W. Wu, *J. Am. Chem. Soc.*, 2012, **134**, 15644-15647.
- 25 T. K. Todorov, J. Tang, S. Bag, O. Gunawan, T. Gokmen, Y. Zhu and D. B. Mitzi, *Adv. Energy Mater.*, 2013, **3**, 34-38.
- 26 S. Lopez-Marino, Y. Sanchez, M. Placidi, A. Fairbrother, M. Espindola-Rodriguez, X. Fontane, V. Izquierdo-Roca, J. Lopez-Garcia, L. Calvo-Barrio, A. Perez-Rodriguez and E. Saucedo, *Chem. Eur. J.*, 2013, **19**, 14814-14822.
- 27 M. Mousel, T. Schwarz, R. Djemour, T. P. Weiss, J. Sandler, J. C. Malaquias, A. Redinger, O. Cojocar-Miredin, P. Choiand and S. Siebentritt, *Adv. Energy Mater.*, 2013, DOI: 10.1002/aenm.201300543.
- 28 W. Septina, S. Ikeda, A. Kyoraiseiki, T. Harada and M. Matsumura, *Electrochim. Acta*, 2013, **88**, 436-442.
- 29 L. Guo, Y. Zhu, O. Gunawan, T. Gokmen, V. R. Deline, S. Ahmed, L. T. Romankiw and H. Deligianni, *Prog. Photovolt: Res. Appl.*, 2014, **22**, 58-68.
- 30 M. T. Winkler, W. Wang, O. Gunawan, H. J. Hovel, T. K. Todorov and D. B. Mitzi, *Energy Environ. Sci.*, 2014, **7**, 1029-1036.

- 31 J. F. Guillemoles , L. Kronik , D. Chaen , U. Rau , A. Jasanek and H. W. Schock , *J. Phys. Chem. B*, 2000, **104**, 4849-4862.
- 32 In our experience, PV performances of our CZTS solar cells obviously decreased after annealing at temperatures more than 200 °C.
- 33 Y. Takemoto, M. Oshima M, K. Yoshino, K. Toyota, K. Inaba, K. Haga, K. Tokudome, *Jpn. J. Appl. Phys.*,2011, **50**, 088001.
- 34 K. Yoshino, Y. Takemoto, M. Oshima, K. Toyota, K.Inaba, K. Haga and K. Tokudome, *Jpn. J. Appl. Phys.*, 2011, **50**, 040207.
- 35 K. Yoshino, A. Ide, A. Mochihara, S. Ikeda and T. Minemoto, submitted in Renewable Energy.
- 36 P. A. Fernandes, P. M. P.Salome and A. F. Da Cunha, *J. Alloys Compound*, 2011, **509**, 7600-7606.
- 37 P. A. Fernandes,P. M. P.Salome and A. F. Da Cunha, *J. Phys. D: Appl. Phys.*, 2010, **43**, 215403.
- 38 L. S. Price, I. P. Parkin, A. M. E. Hardy and R. J. H. Clark, *Chem. Mater.*, 1999, **11**, 1792-1799.
- 39 K. Inaba, Y. Takemoto, K. Toyota, K-i. Haga, K. Tokudome, M. Shinmiya, N. Kamiya, M. Oshima and K. Yoshino, *Mater. Sci. Forum*, 2012, **725**, 277-280.



**Table 1.** Solar cell parameters of Al/GZO/CdS/CZTS/Mo/glass cells

entry	$J_{SC} / \text{mA cm}^{-2}$	$V_{OC} / \text{mV}$	FF	$\eta / \%$
1	14.1	565	0.517	4.12
2	6.7	196	0.257	0.34
3	16.7	660	0.502	5.54
4	16.9	662	0.552	6.17
5	15.8	592	0.486	4.55
6	16.1	669	0.516	5.56
7	16.6	678	0.571	6.43
8	16.2	691	0.571	6.38

**Figure captions**

**Fig. 1** Cross-sectional SEM images of (a) electrodeposited Cu-Sn-Zn precursor, (b) that annealed at 310°C for 2.5 h in an evacuated ampoule, and (c) the CZTS film obtained by sulfurization of the annealed precursor. (d) Surface SEM image, (e) XRD pattern, and (f) Raman spectrum of the corresponding CZTS film.

**Fig. 2** (a) XRD pattern, (b) cross-sectional SEM image, and (c) optical transmittance spectrum of the GZO film sprayed on the glass substrate. An XRD pattern of ZnO powder is also given in panel (a).

**Fig. 3** (a) cross-sectional SEM image and (b) EQE spectrum of the solar cell with a conversion efficiency of 6.43%.

**TOC text**

Cost effective non-vacuum sprayed GZO layer was firstly utilized in electrodeposited CZTS-based thin film solar cells. The thus-obtained champion solar device presented an appreciable conversion efficiency of 6.43%.